Rectangular Waveguide with T-Shaped Septa

GOPA GUHA MAZUMDER AND PRADIP KUMAR SAHA

Abstract —**Recently, a new rectangular waveguide with two T-shaped septa has been proposed by the authors as a superior alternative to conventional ridged guide. Here, numerical data on the cutoff and bandwidth characteristics of the dominant TE_{10} mode of rectangular waveguide with a single T-septum are presented and compared with those of single-ridged guides. The gap impedances of both the double and single T-septum guides are also determined as functions of gap parameters.**

I. Introduction

RECENTLY, the authors proposed a new type of broad-band rectangular waveguide with double T-shaped septa (DTSG), shown in Fig. 1(a), as an alternative to conventional double-ridged guide (DRG) [1]. The structure was arrived at intuitively. Then, a rigorous analysis using the Ritz–Galerkin technique revealed that the dominant TE_{10} mode of symmetric DTSG can have larger cutoff wavelength and bandwidth than a DRG with identical gap dimensions. Further, the ridge dimensions of a DRG have to be optimized separately for cutoff wavelength and bandwidth, whereas a symmetric DTSG, when its septum dimensions are optimized for bandwidth, can have a cutoff wavelength about 15 percent higher than that of a DRG.

In this paper, the Ritz–Galerkin technique has been applied to a rectangular waveguide with single T-shaped septum (STSG), shown in Fig. 1(b), and its theoretical characteristics have been compared with those of single ridged guide (SRG) with identical gap parameters. In addition, the eigenvectors corresponding to the eigenvalues of the new structures have been solved by iteration of the matrix eigenvalue equations and the results have been used to compute the gap impedance of both DTSG and STSG as function of gap parameters.

II. Theory

The symmetric DTSG, considered here, is shown in Fig. 1(a). For analysis, it is necessary to formulate only the quarter problem (Fig. 1(c)). It may be noted that in the limit $g \to 0$ or $h \to 0$, the septum guide approaches the conventional ridged guide. Only the TE modes are considered in the analysis, since the TM modes are of little importance for practical applications and usual waveguide aspect ratios [2].

As in [1], the modal analysis employs the Ritz–Galerkin technique. Since the details of the steps to arrive at the matrix eigenvalue equation can be found in [1], only the final equations are presented, without intermediate manipulations.

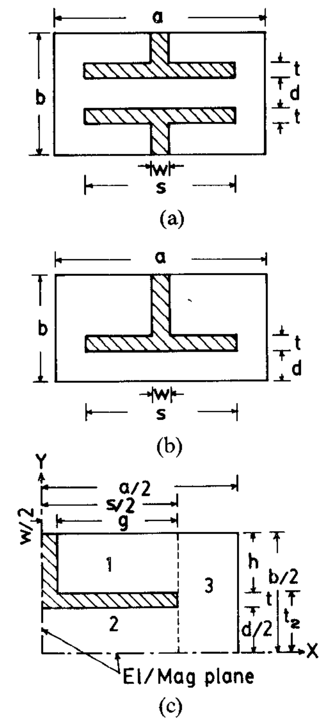

Fig. 1. (a) Rectangular waveguide with symmetric double T-septa (DTSG). (b) Rectangular waveguide with single T-septum (STSG). (c) One quarter of the cross section of doubly symmetric DTSG.

A. Matrix Eigenvalue Equation

The matrix equation for the eigenvalue k_c is found to be of the form

$$[H(k_c)]A = 0. \tag{1}$$

The vector A in (1) is given by

$$A = [A_1^T A_2^T]^T \tag{2}$$

where the superscript T denotes transpose, and the elements of the vectors A_1 and A_2 are the expansion coefficients of the aperture electric fields at $x = s/2$:

$$E_{a1}(y) = \sum_{m=0}^{M} A_{1m} \cos\left(\frac{m\pi}{h}(y - t_2)\right) \qquad (t_2 \leqslant y \leqslant b/2) \tag{3}$$

$$E_{a2}(y) = \sum_{n=0}^{N} A_{2n} \cos\left(\frac{\pi}{d}\begin{Bmatrix} 2n+1 \\ 2n \end{Bmatrix}\left(y - \frac{d}{2}\right)\right) \qquad (0 \leqslant y \leqslant d/2). \tag{4}$$

Manuscript received June 27, 1986; revised September 11, 1986.
The authors are with the Institute of Radiophysics and Electronics, University College of Technology, Calcutta 700 009, India.
IEEE Log Number 8611625.

0018-9480/87/0200-0201$01.00 ©1987 IEEE

The upper and lower integers are for magnetic and electric symmetry, respectively, along the x-axis. The matrix H has the following partitioned form:

$$H=\left[\begin{array}{c|c} H_1 & H_2 \\ \hline H_3 & H_4 \end{array}\right]. \tag{5}$$

The eigenvalue equation is then

$$\det\left[H(k_c)\right]=0 \tag{6}$$

the roots of which yield the TE eigenvalues. The matrix elements are given by the following expressions:

$$H_{1qm}=\sum_{l=0}^{\infty} f_l x_{1ql} x_{1ml} + \delta_{qm}\epsilon_q h \frac{\cot k_{x1q} g}{k_{x1q}} \tag{7}$$

$$H_{2qn}=\sum_{l=0}^{\infty} f_l x_{1ql} x_{2nl} \tag{8}$$

$$H_{3rm}=\sum_{l=0}^{\infty} f_l x_{2rl} x_{1ml} \tag{9}$$

$$H_{4rn}=\sum_{l=0}^{\infty} f_l x_{2rl} x_{2nl} + \delta_{rn}\begin{Bmatrix}2r+1\\ 2r\end{Bmatrix}\frac{d}{2}k_{x2r}^{-1}\begin{Bmatrix}-\tan\\ \cot\end{Bmatrix} k_{x2r}s/2, \tag{10}$$

$$q,m=0,1,\cdots,M$$
$$r,n=0,1,\cdots,N.$$

The upper and lower functions in (10) correspond to magnetic and electric symmetry, respectively, in the gap (region 2) at $x=0$. The other terms are defined as follows:

$$f_l=\frac{\cot k_{x3l}c}{\begin{Bmatrix}\epsilon_{2l}+1\\ \epsilon_{2l}\end{Bmatrix} k_{x3l}b/2} \tag{11}$$

$$\epsilon_p=\begin{cases}1, & p=0\\ 1/2, & p\neq 0\end{cases} \tag{12}$$

$$x_{1_{ij}}=\int_{t_2}^{b/2}\cos\left(\frac{i\pi}{h}(y-t_2)\right)\cos\left(\frac{\pi}{b}\begin{Bmatrix}2j+1\\ 2j\end{Bmatrix}\left(y-\frac{b}{2}\right)\right)dy \tag{13}$$

$$x_{2_{ij}}=\int_{0}^{d/2}\cos\left(\frac{\pi}{d}\begin{Bmatrix}2i+1\\ 2i\end{Bmatrix}\left(y-\frac{d}{2}\right)\right)\cdot\cos\left(\frac{\pi}{b}\begin{Bmatrix}2j+1\\ 2j\end{Bmatrix}\left(y-\frac{b}{2}\right)\right)dy \tag{14}$$

$$k_{x1m}^2+\left(\frac{m\pi}{h}\right)^2=k_c^2, \qquad m=0,1,\cdots \tag{15a}$$

$$k_{x2n}^2+\left(\frac{\pi}{d}\right)^2\begin{Bmatrix}(2n+1)^2\\ (2n)^2\end{Bmatrix}=k_c^2, \qquad n=0,1,\cdots \tag{15b}$$

$$k_{x3l}^2+\left(\frac{\pi}{b}\right)^2\begin{Bmatrix}(2l+1)^2\\ (2l)^2\end{Bmatrix}=k_c^2, \qquad 1=0,1,\cdots. \tag{15c}$$

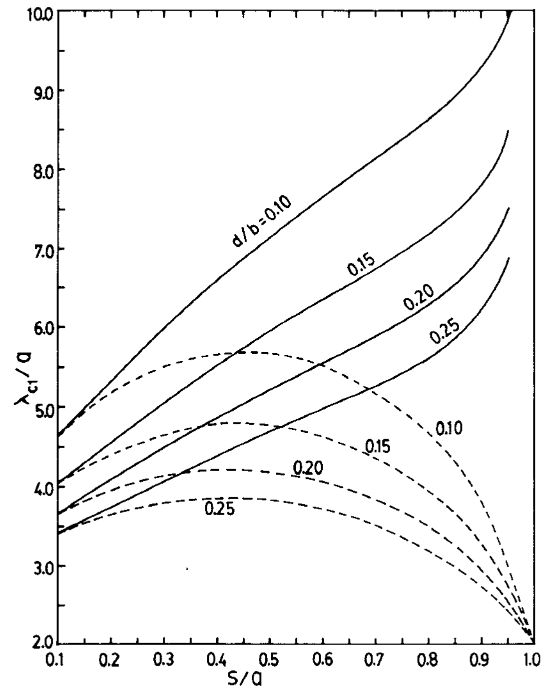

Fig. 2. Variation of normalized cutoff wavelength (λ_{c1}/a) of TE_{10} mode. $b/a=0.45$. —— STSG ($w/a=0.1$, $t/b=0.05$). ---- SRG.

B. Solution of Eigenvector

To solve the eigenvector by iteration, the vectors A_1 and A_2 are first rewritten as

$$A_1=\left[A_{10}A_{1M}^T\right]^T \tag{16a}$$

$$A_2=\left[A_{20}A_{2N}^T\right]^T. \tag{16b}$$

Next, from all the submatrices H_i, $i=1,2,3,4$, the first row and first column are deleted and new submatrices H_{1MM}, H_{2MN}, H_{3MN}, and H_{4NN} are defined. Further, the column vectors H_{1MO}, H_{2MO}, H_{3NO}, and H_{4NO} are defined by deleting the first element of each of the first columns of H_i. Then, the matrix equation (1) can be recast in the following form (suitable for solving A_{1M} and A_{2N} by iteration with A_{10} and A_{20} made arbitrary prior to normalization of the eigenvector A):

$$[H_{1MM}]A_{1M}+[H_{2MN}]A_{2N}=H_{1MO}A_{10}+H_{2MO}A_{20} \tag{17}$$

$$[H_{3NM}]A_{1M}+[H_{4NN}]A_{2N}=H_{3NO}A_{10}+H_{4NO}A_{20}. \tag{18}$$

C. Gap Impedance

The TE_{10} mode gap impedance Z_g of a DTSG is defined as [3]

$$Z_g=V_o^2/2P_o \tag{19}$$

where P_o is the power propagating in the guide, and V_o is the voltage at the center of the gap defined through

$$V_o=-\int_{-d/2}^{d/2} e_y(x=0,y)\,dy. \tag{20}$$

If the basis fields in the expansion of the fields in different regions are made orthonormal, then following [3], Z_g can

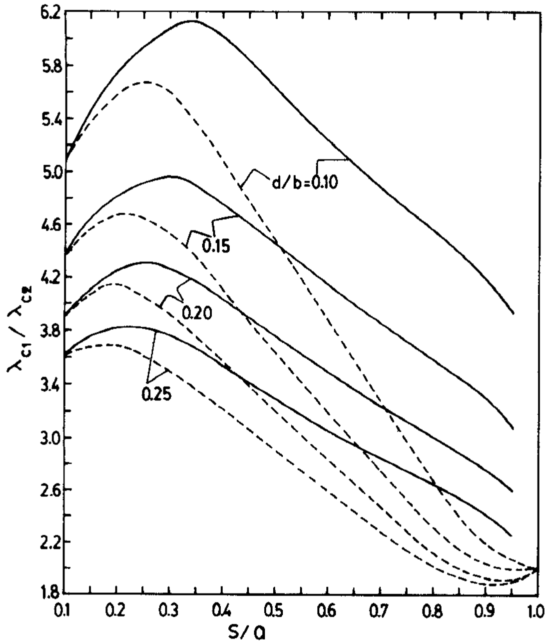

Fig. 3. Bandwidth characteristics: variation of $(\lambda_{c1}/\lambda_{c2})$. $b/a = 0.45$. —— STSG ($w/a = 0.1$, $t/b = 0.05$). ---- SRG.

be defined in terms of A_{20}. At the gap center

$$Z_g = Z_{g(\infty)}\left[1-(\lambda/\lambda_c)^2\right]^{-1/2} \tag{21}$$

where $Z_{g(\infty)}$ is the gap impedance at infinite frequency and is given by

$$Z_{g(\infty)} = \frac{A_{20}^2 d^2}{\cos^2(k_c s/2)} 120\pi. \tag{22}$$

For a STSG with a given aspect ratio b/a and gap ratios d/b and s/a, the gap impedance is obtained by halving that of a DTSG with aspect ratio $2(b/a)$ and the same gap parameters.

III. Numerical Computation and Results

A. Cutoff Wavelength and Bandwidth

The normalized cutoff wavelength λ_{c1}/a of the dominant TE_{10} hybrid mode [3] and the λ_{c2}/a of the next higher order TE_{20} hybrid mode, which determines the bandwidth, were computed from the iterative solution of (6). The l-summation was truncated after $L+1$ terms. For all computations, $N = M = 10$ and $L = 20$ were chosen after studying the eigenvalue convergence [1].

Numerical results show that for a given set of values of the gap parameters d/b and s/a, the largest value of λ_{c1}/a is obtained for $t = w = 0$, that is, for zero-thickness septum. Further, if the septum guide is made to approach a ridged guide by $w \to s$ (or $g \to 0$) or $t \to (b-d)/2$ (or $h \to 0$), the value of λ_{c1}/a decreases monotonically to that of the ridged guide [1].

The variation of λ_{c1}/a and $\lambda_{c1}/\lambda_{c2}$ of a STSG with $b/a = 0.45$ is shown in Figs. 2 and 3, respectively. The chosen values of septum thickness ratios are $t/b = 0.05$ and $w/a = 0.1$. Also shown in the figures are the corresponding characteristics of a conventional single-ridged guide with the same b/a. In computations, the values of b/a were chosen to be 0.5 and 0.45 for DTSG and STSG, respectively, since the DRG and SRG data for these values of b/a are readily available [4] for comparison.

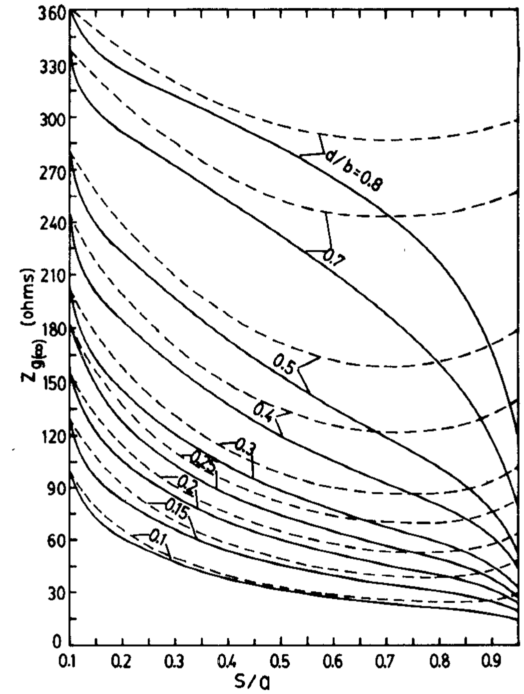

Fig. 4. Variation of gap impedance $Z_{g(\infty)}$. $b/a = 0.5$. —— DTSG ($w/a = 0.1$, $t/b = 0.05$). ---- DRG.

The cutoff and bandwidth characteristics of DTSG and STSG are found to be similar. For both types of T-septum guides, λ_{c1}/a increases with s/a and can have a much larger value than that of a ridged waveguide with the same gap parameters. The bandwidth peaks are also higher and occur at higher vlaues of s/a. Beyond the peaks, the bandwidth falls off less rapidly and remains larger than that of a ridged waveguide.

Evidently, the T-septa provide higher capacitive loading than the solid ridges, and this loading increases as the septum width s increases at a fixed gap width d. A ridged waveguide, for $s/a = 1$, reduces to a hollow rectangular waveguide with a different aspect ratio. In the case of T-septum guides, however, $s/a = 1$ does not yield a meaningful guiding structure since the field in region 1 is nonzero. This limiting case is therefore excluded from the parameter values in computations.

B. Gap Impedance

For determining the eigenvector A corresponding to the eigenvalue k_c of the TE_{10} mode, the Gauss–Siedel iteration scheme was employed to solve (17) and (18). A_{20} was made unity and A_{10} varied to minimize the norm of the computed vector $[H]\,A$. The eigenvector was then normalized and $Z_{g(\infty)}$ computed from (22) as a function of d/b and s/a. The variation of gap impedance of DTSG and STSG is shown in Figs. 4 and 5, respectively. The $Z_{g(\infty)}$ of SRG, obtained from the design curves in [4], and that of

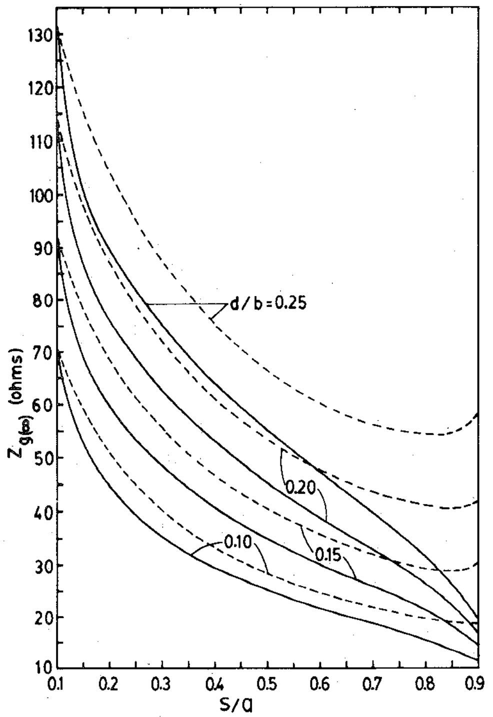

Fig. 5. Variation of gap impedance $Z_{g(\infty)}$. $b/a = 0.45$. —— STSG ($w/a = 0.1$, $t/b = 0.05$). ---- SRG.

DRG, calculated from Hopfer's expression [5], are also shown in the figures for comparison. The $Z_{g(\infty)}$ of the septum guides coincides with that of ridged guides when $s/a = w/a = 0.1$ and for higher values of s/a remains lower than that of ridged guides. It also covers a wider range of impedance values for moderate to large values of gap width d/b.

IV. Summary

A new type of rectangular waveguide with two symmetric T-shaped septa has been analyzed by the Ritz–Galerkin technique and is found to have a broader range of parameters than conventional ridged guides. The cutoff and bandwidth characteristics of the TE_{10} mode of this structure has been reported in [1].

Here, the characteristics of a structure with single T-septum have been presented. Though an experimental verification of the theoretical results is yet to be carried out, these appear to be correct from the comparison with the special case of ridged waveguides. Further design data are provided by presenting the gap impedance of both types of structures as a function of gap parameters. The wide range of gap impedance shown by the structures indicates that steps in the septum width s alone, at a fixed gap width d, may be used for impedance transformation. It is proposed that for continuous transition to rectangular waveguide, a taper in the septum width from s to w be followed by a taper in the septum height to zero.

Fabrication of a septum guide would obviously be more difficult than a ridged guide, but its advantages should outweigh this drawback. An excellent guideline for making a test structure can be obtained from Elliot's paper [6] on a two-mode equal-velocity T-septum waveguide.

Acknowledgment

The authors are thankful to Prof. B. R. Nag for his interest and encouragement. The critical appraisal of a reviewer has been of immense help in revising the manuscript.

References

[1] G. G. Mazumder and P. K. Saha, "A novel rectangular waveguide with double T-septums," *IEEE Trans. Microwave Theory Tech.*, vol. MTT-33, pp. 1235–1238, Nov. 1985.

[2] G. Magerl, "Ridged waveguides with inhomogeneous dielectric slab loading," *IEEE Trans. Microwave Theory Tech.*, vol. MTT-26, pp. 413–416, June 1978.

[3] J. P. Montgomery, "On complete eigenvalue solution of ridged waveguide," *IEEE Trans. Microwave Theory Tech.*, vol. MTT-19, pp. 547–555, June 1971.

[4] T. S. Saad, Ed., *Microwave Engineers' Handbook*, vol. 1. Dedham, MA: Artech House, 1971, pp. 87–89.

[5] S. Hopfer, "The design of ridged waveguides," *IRE Trans. Microwave Theory Tech.*, vol. MTT-3, pp. 20–29, Oct. 1955.

[6] R. S. Elliot, "Two-mode waveguide for equal mode velocities," *IEEE Trans. Microwave Theory Tech.*, vol. MTT-16, pp. 282–286, May 1968.

Gopa Guha Mazumder was born in 1957. She completed the B.Sc. (with honors) in 1976 and the B.Tech. and M.Tech. in radiophysics and electronics in 1979 and 1982, respectively, all at the University of Calcutta. She is now working toward the Ph.D. degree. Her field of interest is microwave and millimeter-wave transmission lines.

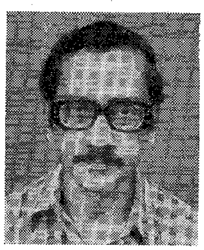

Pradip Kumar Saha received the B.Sc. (with honors) in physics in 1963 and the M.Tech. in radiophysics and electronics in 1966, both from the University of Calcutta. In 1970, he received the Ph.D. degree from the University of Leeds, England.

He has been on the teaching staff of the Institute of Radiophysics and Electronics at the University of Calcutta since 1971. Dr. Saha has worked in the field of microwave antennas and he is currently engaged in the fields of microwave and millimeter-wave transmission lines, microwave semiconductor devices, and power sources.